Distributed Coordination of Household Electricity Consumption

Morten Juelsgaard, *student member IEEE,* André Teixeira, Mikael Johansson, *member IEEE,* Rafael Wisniewski, *member IEEE,* Jan Bendtsen, *member IEEE*

***Abstract*— This work presents a distributed framework for coordination of flexible electricity consumption for a number of households in the distribution grid. Coordination is conducted with the purpose of minimizing a trade-off between individual concerns about discomfort and electricity cost, on the one hand, and joint concerns about grid losses and voltage variations on the other. Our contribution is to demonstrate how distributed coordination of both active and reactive consumption may be conducted, when consumers are jointly coupled by grid losses and voltage variations. We further illustrate the benefit of including consumption coordination for grid operation, and how different types of consumption present different benefits.**

I. Introduction

Previous works have shown how several types of electrical power consumption is highly flexible in the sense that it may be temporally shifted with little or no discomfort to the consumer [1]–[4]. Proper utilization of this flexibility, through coordination of consumption, may be used to minimize grid losses, control voltage, avoid grid congestion, *etc*. This comprises the focus of this work.

The information required to conduct coordination may encompass sensible information about each consumer. Such information should be kept private, which requires a coordination framework allowing this information to remain private and distributed among each individual consumer, rather than requiring the information to be collected and stored centrally.

Previous works on distributed consumption coordination include [3], [5], [6]. The work by [3] took into account the behavior of consumers to coordinate consumption of active power in a simplified grid. The coordination reduced cost of losses, but disregarded voltage variations. In [5] the consumer behavior was similarly used for active power coordination in a more general and detailed grid structure, however, while also disregarding voltage drops. The work in [6] managed voltage drops and power losses by optimizing *reactive* power flow in grids with line topology, but disregarded active power management and omitted any concerns towards consumer behavior.

This work performs joint coordination of active *and* reactive power consumption, such as to account for both private consumer concerns, cost of transport losses *and* voltage quality throughout the grid. That is, this works extends the results of the works cited above, by solving a combined problem, thus expanding the complexity of the previously treated problems.

The first, fourth and fifth authors are with the Department of Automation and Control, Aalborg University, Denmark. The second and third authors are with the ACCESS Linnaeus Center, Automatic Control Lab., KTH, Sweden. Contact (corresponding author): mju@es.aau.dk

Our work relies on the known method of Alternating Direction Method of Multipliers (ADMM) [7] for distributed coordination, and follows an approach similar to [5]; however, our distributed framework is extended to include voltage variations as well as cost of transport losses in the grid. The contribution of this work lies not in the derivation of the theoretical methods, but in extending previous formulations of an intricate problem relating to electrical grid operation, and demonstrating how it may still be solved in a distributed fashion, using available techniques. For this, we consider a future electrical grid with advanced metering and control infrastructure that allows each consumer, cable, and grid junction, to play an active part in the coordination.

The remainder of this paper is organized as follows. Section II presents the models required to formally state the coordination problem in Section III. The ADMM framework for solving the coordination in a distributed fashion is presented in Section IV, for which a numerical example is presented in Section V. Final remarks and perspectives are provided in Section VI.

II. Modeling

The following is divided into an outline of the grid structure, a derivation of the grid model and a derivation of the consumer models.

A. Grid structure

Our focus is low-voltage distribution grids, as illustrated in Fig. 1.

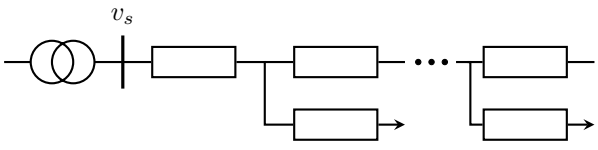

Fig. 1. Low voltage grid and the associated grid components.

The grid consists physically of a transformer substation (⊚), cable sections (⊣□⊢), and consumer connection points (↓). The links in between cables, as well as between cables and consumers, represent grid junctions, also referred to as bus-bars. The bus-bar at the secondary side of the transformer, indicated with a vertical line, is considered a slack-bus [8], with fixed normalized voltage magnitude $v_s = 1$ pu. In addition, we assume that the grid is balanced, allowing the analysis to be performed for an equivalent single phase system.

We represent the network layout as a connected, undirected graph where cable sections, represented by impedances, compose the edges and bus-bars compose the

nodes. Consumers are connected to the network through a single private cable section. This gives a natural sub-division of cables into two categories; leaves, comprising the private cable of each consumer, and branches, comprising shared cables. Let the network contain $n \in \mathbf{N}$ consumers and $b \in \mathbf{N}$ branch cables. This means that the network contains $n+b$ bus-bars, excluding the secondary transformer side. We define sets

$$\mathcal{I} = \{1, \ldots, n\}, \quad \mathcal{J} = \{1, \ldots, n+b\},$$

and assign an ordering to the network components as follows: leaves and consumers are numbered by $i \in \mathcal{I}$, such that leaves are assigned the same number as the consumer it connects. Branches are numbered $j \in \{n+1, \ldots, n+b\}$.

To make the exposition clearer throughout, we limit our attention to networks whose graphs compose a tree, rooted at the transformer, although our results can be generalized to any connected, undirected graphs. We define mappings

$$\text{Pa}(j) \in \mathcal{J}, \quad \text{Ch}(j) \subset \mathcal{J}, \quad j \in \mathcal{J}$$

denoting the unique parent edge, and the set of children edges of each cable, in a graph-theoretical sense.

B. Grid modeling

The distribution cables are modeled as RL-series circuits. More general π-models could be used however, since we study low-voltage distribution grids, each cable section is considered to be short, and shunt capacitances are thus neglected. Nonetheless, the derivations in this section can be repeated including shunt capacitances, whereby corresponding although more complicated equations would be obtained.

Each cable section is modeled as an impedance $z_j = r_j + \mathrm{j}x_j \in \mathbf{C}$, with $j \in \mathcal{J}$ and $r_j, x_j > 0$ being the resistance and reactance of each cable section, respectively [8]. Consider an isolated cable $j \in \mathcal{J}$ illustrated in Fig. 2.

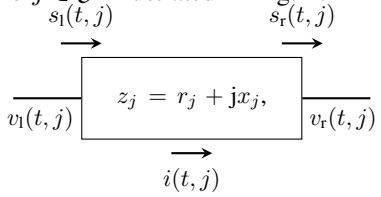

Fig. 2. Illustration of an isolated grid section, including the power flow through the two terminals.

In the terminology of [5], each cable section is considered a two-terminal device, and we introduce the map $s_{\mathrm{l}} : \mathcal{T} \times \mathcal{J} \to \mathbf{C}$ to denote the left-terminal complex power, where $\mathcal{T} = \{1, 2, \ldots, N\}$ is a discrete coordination horizon of N steps. Similar to $s_{\mathrm{l}}(t,j)$ we define $s_{\mathrm{r}}(t,j), t \in \mathcal{T}, j \in \mathcal{J}$ as the right-terminal power. We extend the notation such that

$$s_{\mathrm{l}}(t,j) = s_{\mathrm{l},j}(t) = s_{\mathrm{l},t}(j) \in \mathbf{C}, \quad \forall j \in \mathcal{J}, t \in \mathcal{T}.$$

Additionally, we generalize this notation such that

$$s_{\mathrm{l},j} = (s_{\mathrm{l}}(1,j), \ldots, s_{\mathrm{l}}(N,j)) \in \mathbf{C}^{|\mathcal{T}|}, \quad j \in \mathcal{J},$$
$$s_{\mathrm{l},t} = (s_{\mathrm{l}}(t,1), \ldots, s_{\mathrm{l}}(t,n+b)) \in \mathbf{C}^{|\mathcal{J}|}, \quad t \in \mathcal{T}.$$

We employ this notation for all similar mappings.

The voltage on either side of the cable section and the current through it are denoted $v_{\mathrm{l}}(t,j), v_{\mathrm{r}}(t,j), i(t,j) \in \mathbf{C}$, respectively.

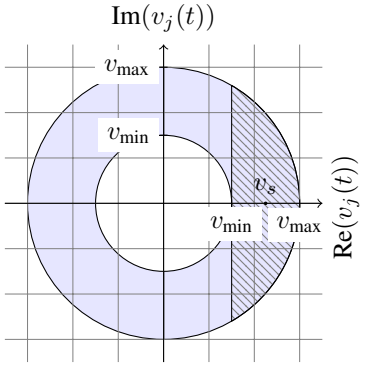

Fig. 3. **Shaded:** The annulus representing the feasible voltage region $\forall j \in \mathcal{J}, \forall t \in \mathcal{T}$. **Hatched:** A convex operating subset ($\mathcal{V}$) of the voltage.

Voltage drop

The current through the cable is [9]:

$$i_j(t) = \left(\frac{s_{\mathrm{l},j}(t)}{v_{\mathrm{l},j}(t)}\right)^* = \left(\frac{s_{\mathrm{r},j}(t)}{v_{\mathrm{r},j}(t)}\right)^*, \tag{1}$$

where $(\cdot)^*$ denotes complex conjugate. The voltage difference across the section is

$$v_{\mathrm{l},j}(t) - v_{\mathrm{r},j}(t) = z_j i_j(t) \quad \Leftrightarrow \quad v_{\mathrm{r},j}(t) = v_{\mathrm{l},j}(t) - z_j i_j(t).$$

Inserting (1) and the impedance expression gives

$$v_{\mathrm{r},j}(t) = v_{\mathrm{l},j}(t) - (r_j + \mathrm{j}x_j)\left(\frac{s_{\mathrm{l},j}(t)}{v_{\mathrm{l},j}(t)}\right)^*. \tag{2}$$

Power quality requirements state that the voltage must be within maximum and minimum magnitudes $v_{\min}, v_{\max} \in \mathbf{R}$ at all times, *i.e.*,

$$v_{\min} \leq |v_{\mathrm{r}}(t,j)| \leq v_{\max}, \quad \forall j \in \mathcal{J}, t \in \mathcal{T} \tag{3}$$

as illustrated in Fig. 3. The specific limits enforced in various countries may vary, however, they would typically be around ± 10 % around the transformer voltage. It is common to operate the electrical grid with a small phase-shift of the voltage [5], effectively tightening the constraint in (3). From this, we reformulate (3) to the hatched convex region of Fig. 3, denoted $\mathcal{V}$. For this tighter constraint, where $v_{\mathrm{r},j}(t), v_{\mathrm{l},j}(t) \in \mathcal{V}$, we approximate $v^*_{\mathrm{l},j}(t) \approx 1$, whereby (2) reduces to

$$v_{\mathrm{r},j}(t) = v_{\mathrm{l},j}(t) - (r_j + \mathrm{j}x_j)s^*_{\mathrm{l},j}(t) \tag{4}$$

The reader should notice from Fig. 1, that $v_{\mathrm{l},j}(t) = v_{\mathrm{r,Pa}(j)}(t)$, and thus

$$v_{\mathrm{r},j}(t) = v_{\mathrm{r,Pa}(j)}(t) - (r_j + \mathrm{j}x_j)s^*_{\mathrm{l},j}(t), \quad \forall j \in \mathcal{J}. \tag{5}$$

We may write (5) more compactly by defining $P \in \{0,1\}^{b \times b}$, and $D_{\mathrm{p}}, D_{\mathrm{q}} \in \mathbf{C}^{b \times b}$ as

$$[P]_{i,j} = \begin{cases} 1, & \text{Pa}(j) = i \\ 0, & \text{otherwise} \end{cases}, \quad [D_{\mathrm{p}}]_{i,j} = \begin{cases} r_j + \mathrm{j}x_j, & i = j \\ 0, & \text{otherwise} \end{cases},$$

and $D_q = -\mathrm{j}D_p$, whereby (5) may be written

$$v_{\mathrm{r},t} = P v_{\mathrm{r},t} - D_{\mathrm{p}}\mathrm{Re}(s_{\mathrm{l},t}) - D_{\mathrm{q}}\mathrm{Im}(s_{\mathrm{l},t}), \quad t \in \mathcal{T}.$$

Losses and cost

From (1), the squared current magnitude is:

$$|i_j(t)|^2 = \frac{|s_{\mathrm{l},j}(t)|^2}{|v_{\mathrm{l},j}(t)|^2} = \frac{|s_{\mathrm{r},j}(t)|^2}{|v_{\mathrm{r},j}(t)|^2} = \frac{1}{2}\left(\frac{|s_{\mathrm{l},j}(t)|^2}{|v_{\mathrm{l},j}(t)|^2} + \frac{|s_{\mathrm{r},j}(t)|^2}{|v_{\mathrm{r},j}(t)|^2}\right).$$

However, as argued above, the voltage constraint entails that $|v_{\mathrm{r},j}(t)| \approx |v_{\mathrm{l},j}(t)| \approx 1, j \in \mathcal{J}, t \in \mathcal{T}$, *i.e.*,

$$|i_j(t)|^2 \approx \frac{1}{2}\left(|s_{\mathrm{l},j}(t)|^2 + |s_{\mathrm{r},j}(t)|^2\right). \tag{6}$$

The active losses are given by $\mathrm{Re}(i_j(t)z_j i_j(t)^*) = r_j|i_j(t)|^2$, and the reactive losses are correspondingly $\mathrm{Im}(i_j(t)z_j i_j(t)^*) = x_j|i_j(t)|^2$. By defining $l : \mathbf{C}^N \times \mathbf{C}^N \to \mathbf{R}^N$ as

$$l(u,y)(t) = \frac{1}{2}\left(|u(t)|^2 + |y(t)|^2\right), \quad t \in \mathcal{T} \tag{7}$$

for any $u, y \in \mathbf{C}^N$, the combined active and reactive losses may be expressed as $z_j l(s_{\mathrm{l},j}, s_{\mathrm{r},j})$, for each cable $j \in \mathcal{J}$. As these losses represents power dissipated in each cable, the physical relation between left and right terminal power flow, is given by

$$s_{\mathrm{l},j} = s_{\mathrm{r},j} + z_j l(s_{\mathrm{l},j}, s_{\mathrm{r},j}), \quad j \in \mathcal{J}. \tag{8}$$

In the sequel, we shall seek to implement the coordination procedure using convex optimization tools. However, since (8) represents a quadratic equality, it is a non-convex constraint. In [5] the convex relaxation

$$s_{\mathrm{l},j}(t) - s_{\mathrm{r},j}(t) \geq z_j l(s_{\mathrm{l},j}, s_{\mathrm{r},j}), \quad j \in \mathcal{J}, \tag{9}$$

was suggested, and it was argued that in tree-networks, the relaxation would be tight.

To define a cost of losses, we introduce a fixed, known estimate of the electricity price $w \in \mathbf{R}^N$, and define $c_l : \mathcal{J} \times \mathbf{C}^N \times \mathbf{C}^N \to \mathbf{R} \cup \{\infty\}$

$$c_{\mathrm{l}}(j,u,y) = \begin{cases} r_j\langle w, \mathrm{Re}(u-y)\rangle, & u \geq y + z_j l(u,y) \\ +\infty, & \text{otherwise,} \end{cases} \tag{10}$$

where $\langle\cdot,\cdot\rangle$ denotes inner product. The estimated cost of the losses in each cable can then be represented as $c_{\mathrm{l}}(j, s_{\mathrm{l},j}, s_{\mathrm{r},j})$, where (9) are implicitly included as an operating constraint.

Bus-bar power conservation

Power conservation throughout the grid entails that the net in- and outflow of power at each node, must coincide. Since we focus on tree structured networks, this is written as

$$s_{\mathrm{r},j} = \sum_{h \in \mathrm{Ch}(j)} s_{\mathrm{l},h}, \quad j \in \mathcal{J}. \tag{11}$$

C. Household consumption

Each consumer $i \in \mathcal{I}$ draws a complex power $s_{\mathrm{c},i}(t) = p_{\mathrm{c},i}(t) + \mathrm{j}q_{\mathrm{c},i}(t) \in \mathbf{C}$, where $p_{\mathrm{c},i}(t), q_{\mathrm{c},i}(t) \in \mathbf{R}$ represent the average active and reactive consumption during $t \in \mathcal{T}$. Let each period $t \in \mathcal{T}$ be of length T_{s}, where the average power $p_{\mathrm{c},i}(t)$ is equivalent to an energy $T_{\mathrm{s}}p_{\mathrm{c},i}(t)$.

Recall that consumers are connected to the grid through a private leaf cable. From the grid ordering defined in Section II-A, this entails

$$s_{\mathrm{r},i} = s_{\mathrm{c},i}, \quad i \in \mathcal{I}.$$

Not all consumption is flexible, so we let

$$p_{\mathrm{c},i}(t) = \tilde{p}_{\mathrm{c},i}(t) + \overline{p}_{\mathrm{c},i}(t), \quad \text{and} \quad q_{\mathrm{c},i}(t) = \tilde{q}_{\mathrm{c},i}(t) + \overline{q}_{\mathrm{c},i}(t),$$
$$\tilde{s}_{\mathrm{c},i}(t) = \tilde{p}_{\mathrm{c},i}(t) + \mathrm{j}\tilde{q}_{\mathrm{c},i}(t), \quad \text{and} \quad \overline{s}_{\mathrm{c},i}(t) = \overline{p}_{\mathrm{c},i}(t) + \mathrm{j}\overline{q}_{\mathrm{c},i}(t),$$

such that $s_{\mathrm{c},i}(t) = \tilde{s}_{\mathrm{c},i}(t) + \overline{s}_{\mathrm{c},i}(t)$, where $\overline{p}_{\mathrm{c},i}(t), \overline{q}_{\mathrm{c},i}(t) \in \mathbf{R}$ represents the estimated inflexible consumption, which cannot be shifted. We refer to this as the baseline consumption. Conversely, $\tilde{p}_{\mathrm{c},i}(t), \tilde{q}_{\mathrm{c},i}(t) \in \mathbf{R}$ represents the flexible consumption, allowing for some degree of temporal shifts.

D. Discomfort and Appliance Constraints

The flexibility of a consumer, depends on the installed appliances and any discomfort and constraints associated to their use. We focus on the flexibility introduced by three generic appliances: electric heat pumps (EHPs), electric vehicles (EVs) and photo-voltaic (PV) arrays. For simplicity, we do not include consumers with more than one appliance, although our approach directly allows for this.

Electric heat pump installed

Let $\mathcal{I}_{\mathrm{ehp}} \subset \mathcal{I}$ be consumers with an EHP installed. For $i \in \mathcal{I}_{\mathrm{ehp}}$ we introduce a state $x_i(t) \in \mathbf{R}$, representing the temperature of the household. A simple thermal model can be approximated as in [1], by a linear first order model:

$$x_i(t+1) = a_i x_i(t) + b_i \tilde{p}_{\mathrm{c},i}(t) + \delta_i(t), \quad i \in \mathcal{I}_{\mathrm{ehp}} \tag{12}$$

where $a_i \in (0,1), b_i \in \mathbf{R}_+$ are estimated model parameters and $\delta_i(t) \in \mathbf{R}$ is an estimate of the disturbance from ambient conditions. We let

$$x_i = (x_i(1), \ldots, x_i(N)) \in \mathbf{R}^N,$$

and consider x_i as a mapping: $x_i : \mathbf{C}^N \to \mathbf{R}^N$, taking the power $\tilde{s}_c$ to the temperature $x_i(\tilde{s_c})$, for $i \in \mathcal{I}_{\mathrm{ehp}}$.

To model comfort of a consumer employing an EHP, we introduce a known set-point $x_{\mathrm{sp},i} \in \mathbf{R}^N$, to which the indoor temperature preferably should remain close, and deviations are translated as a discomfort of the consumer. From this, we define the discomfort $\overline{d}_i : \mathbf{C}^N \to \mathbf{R}$, as

$$\overline{d}_i(\tilde{s}_{\mathrm{c},i}) = \|x_i(\tilde{s}_{\mathrm{c},i}) - x_{\mathrm{sp},i}\|_2^2, \quad i \in \mathcal{I}_{\mathrm{ehp}}. \tag{13}$$

The operation of the heat pump is bounded by upper and lower limits of the consumption, such that

$$\underline{p}_{\mathrm{ehp},i} \leq \tilde{p}_{\mathrm{c},i}(t) \leq \overline{p}_{\mathrm{ehp},i}, \quad t \in \mathcal{T}, \tag{14}$$

where $\underline{p}_{\mathrm{ehp},i}, \overline{p}_{\mathrm{ehp},i} \in \mathbf{R}$ are known operating limits. We further enforce limits on temperature $\underline{x}_{\mathrm{ehp},i}, \overline{x}_{\mathrm{ehp},i} \in \mathbf{R}$, such that

$$\underline{x}_{\mathrm{ehp},i} \leq x_i(\tilde{s}_{\mathrm{c},i}) \leq \overline{x}_{\mathrm{ehp},i}, \tag{15}$$

where the inequalities above are to be read entry-wise.

Finally, in this work the flexibility of the EHP is solely related to the consumption of active power, *i.e.*, there is no flexibility for reactive consumption, so $\tilde{q}_{\mathrm{c},i}(t) = 0, t \in \mathcal{T}$.

Provided known parameters in the model of (12), we collect the constraints in the set

$$\mathcal{S}_i = \{\tilde{s} = \tilde{p} + \mathrm{j}\tilde{q} \mid \underline{p}_{\mathrm{ehp},i} \leq \tilde{p}(t) \leq \overline{p}_{\mathrm{ehp},i},\ \tilde{q} = 0$$
$$\underline{x}_{\mathrm{ehp},i} \leq x_i(\tilde{s}) \leq \overline{x}_{\mathrm{ehp},i}\} \subset \mathbf{C}^{|\mathcal{T}|},$$

for $i \in \mathcal{I}_{\text{ehp}}$. For brevity of notation, we shall include these private constraints implicitly in the discomfort of the consumer, by defining the extended value discomfort as

$$d_i(\tilde{s}) = \begin{cases} \overline{d}_i(\tilde{s}), & \tilde{s} \in \mathcal{S}_i \\ +\infty, & \text{otherwise.} \end{cases} \tag{16}$$

for any $\tilde{s} \in \mathbf{C}^{|\mathcal{T}|}$ and $i \in \mathcal{I}_{\text{ehp}}$. We use a similar notation onwards for the remaining appliances.

Electric vehicle installed

Let $\mathcal{I}_{\text{ev}} \subset \mathcal{I}$ denote households with EVs installed. The EV charging is not subject to a setpoint or preferred charge schedule. Instead the vehicle is required to be charged completely during the horizon, *i.e*.

$$\sum_{t \in \mathcal{T}} T_{\text{s}} \tilde{p}_{\text{c},i}(t) = e_{\text{dem},i}, \tag{17}$$

for some demand $e_{\text{dem},i} > 0$. Additionally, the vehicle must, similarly to the EHP, obey limits on charge and storage capacity

$$\underline{p}_{\text{ev},i} \leq \tilde{p}_{\text{c},i}(t) \leq \overline{p}_{\text{ev},i}, \;\; \underline{e}_{\text{ev},i} \leq \sum_{t=1}^{\tau} T_{\text{s}} \tilde{p}_{\text{c},i}(t) \leq \overline{e}_{\text{ev},i}, \;\; \forall \tau \in \mathcal{T} \tag{18}$$

with limits $\underline{p}_{\text{ev},i}, \overline{p}_{\text{ev},i}, \underline{e}_{\text{ev},i}, \overline{e}_{\text{ev},i} \in \mathbf{R}$. The vehicle will typically be away from the charging station for some period every day, where it cannot be charged, *i.e*,

$$\tilde{p}_{\text{c},i}(t) = 0, \quad \forall t \in \{\tau \mid \tau \in \mathcal{T}, \tau \leq t_{\text{ev},i}\}. \tag{19}$$

where $t_{\text{ev},i} \in \mathcal{T}$ denote an estimate of the time-of-plug-in.

It has been argued that the inverter based consumption such as EVs are capable of both supplying and consuming reactive power [10]. The constraint is here that the capacity of the inverter must not be exceeded:

$$\tilde{q}_{\text{c},i}(t)^2 + \tilde{p}_{\text{c},i}(t)^2 \leq \overline{s}_{\text{ev},i}^2, \quad t \in \mathcal{T}, \tag{20}$$

where $\overline{s}_{\text{ev},i} > 0$ is an upper limit of the apparent power of the inverter.

Collecting the constraints in (17), (18), (19), (20), the feasible operating set of an EV is

$$\begin{aligned} \mathcal{S}_i = \{\tilde{s} = \tilde{p} + \text{j}\tilde{q} \mid \; & \textstyle\sum_{\tau \in \mathcal{T}} T_{\text{s}} \tilde{p}(\tau) = e_{\text{dem},i}, \; \underline{p}_{\text{ev},i} \leq \tilde{p}(t) \leq \overline{p}_{\text{ev},i}, \\ & \underline{e}_{\text{ev},i} \leq \textstyle\sum_{\tau=1}^{t} T_{\text{s}} \tilde{p}_i(\tau) \leq \overline{e}_{\text{ev},i}, \; t \in \mathcal{T} \\ & \tilde{p}(\tau) = 0, \tau \leq t_{\text{ev},i}, \; \tilde{q}(t)^2 + \tilde{p}(t)^2 \leq s_{\text{ev},i}^2\} \subset \mathbf{C}^{|\mathcal{T}|}. \end{aligned}$$

As any charge schedule fulfilling these constraints are equally acceptable, the discomfort is $\overline{d}_i(\tilde{s}) = 0, i \in \mathcal{I}_{\text{ev}}$.

Photo-voltaics installed

Let $\mathcal{I}_{\text{pv}} \subset \mathcal{I}$ denote consumers with solar panels installed. The active consumption of a PV array is governed by weather conditions, and cannot be controlled, *i.e*. $\tilde{p}_{\text{c},i}(t) = \overline{p}_{\text{pv},i}(t), \forall i \in \mathcal{I}_{\text{pv}}, t \in \mathcal{T}$, where $\overline{p}_{\text{pv},i}(t) \in \mathbf{R}_+$ denotes some estimate of the solar production.

As PVs are inverter based, similar reactive capabilities applies as for EVs [11]:

$$\tilde{q}_{\text{c},i}(t)^2 + \overline{p}_{\text{pv},i}(t)^2 \leq \overline{s}_{\text{pv},i}^2,$$

where $\overline{s}_{\text{pv},i} > 0$ is an upper limit of the apparent power of the inverter. The constraints can be collected as

$$\mathcal{S}_i = \{\tilde{s} = \tilde{p} + \text{j}\tilde{q} \mid \tilde{p} = \overline{p}_{\text{pv},i}, \tilde{q}(t)^2 + \overline{p}_{\text{pv},i}(t)^2 \leq \overline{s}_{\text{pv},i}^2\} \subset \mathbf{C}^{|\mathcal{T}|}.$$

Similar to the case of the EVs, there is no discomfort related to employing the flexibility of PVs, so $\overline{d}_i(\tilde{s}) = 0$.

E. Household objective

The objective of each household is to minimize the discomfort, as a trade-off with minimizing the cost of buying electricity. Additionally, recall that each consumer is connected to the grid through a private leaf-cable and that $s_{\text{r},i} = s_{\text{c},i}$, $i \in \mathcal{I}$. The power transported through the leaf is thus defined solely by the consumer, and so are the losses introduced in the leaf. We therefore assign the cost of losses in each leaf, specifically to the individual consumer connected through it.

Given the price estimate introduced earlier, the estimated cost of buying electricity, the cost of leaf losses and the discomfort for each consumer is

$$c_{\text{e}}(i, s_{\text{l},i}, s_{\text{c},i}) = \langle w, \text{Re}(s_{\text{c},i}) \rangle + c_{\text{l}}(i, s_{\text{l},i}, s_{\text{c},i}) + \lambda_i d_i(\tilde{s}_{\text{c},i}),$$

for $i \in \mathcal{I}$, where $\lambda_i > 0$ is a trade-off parameter private to each consumer. The cost of energy is only related to the active consumption, *i.e*. no monetary cost is directly introduced from the reactive power consumption.

III. Coordination problem

The primary task of the coordination is to ensure that the constraints of the grid and each individual consumer are satisfied.

The secondary task of coordination is to achieve a trade-off between the consumers cost of energy and discomfort, as well as the cost of losses incurred in the grid. Given the models discussed in Section II, this problem is stated as

Problem 1 (Centralized problem):
Provided:

- mappings c_{e}, and c_{l}
- grid structure $\text{Pa}(j), \text{Ch}(j), j \in \mathcal{J}$
- matrices $P, D_{\text{p}}, D_{\text{q}}$
- set $\mathcal{V}$

Solve:

$$\begin{aligned} \underset{\substack{s_{\text{c},i}, s_{\text{l},j}, s_{\text{r},j}, u_{\text{r},j} \\ i \in \mathcal{I}, j \in \mathcal{J}}}{\text{minimize}} \quad & \sum_{i \in \mathcal{I}} c_{\text{e}}(i, s_{\text{l},i}, s_{\text{c},i}) + \sum_{j \in \mathcal{J} \setminus \mathcal{I}} c_{\text{l}}(j, s_{\text{l},j}, s_{\text{r},j}) \\ \text{subject to} \quad & v_{\text{r},t} = P v_{\text{r},t} - D_{\text{p}} \text{Re}(s_{\text{l},t}) - D_{\text{q}} \text{Im}(s_{\text{l},t}) \\ & v_{\text{r},t} \in \mathcal{V}, \quad s_{\text{r},j} = \textstyle\sum_{h \in \text{Ch}(j)} s_{\text{l},h}, \end{aligned} \tag{21}$$

for $t \in \mathcal{T}$, with the implicit constraint $s_{\text{c},i} = s_{\text{r},i}, i \in \mathcal{I}$. The optimal cost of (21) is denoted $\phi^\star \in \mathbf{R}$.

Given the approximations introduced in Section II, (21) is a convex problem. To see this, notice that each component of the objective function is convex in the real and imaginary parts of the variables, separately. The same holds for all constraints in (21).

We assume that Problem 1 is strictly feasible, *i.e*., that there exists consumption profiles for each consumer that would be strictly within their individual private constraints, as well as strictly satisfy the grid constraints.

A. Benchmark strategy

Before deriving the distributed approach for solving Problem 1, we shall initially derive a benchmark strategy to be used for comparison in the numerical example in Section V. In this strategy, each consumer only considers private objectives and constraints, and disregards any joint objectives and constraints. The strategy can be formulated through the following problem:

Problem 2 (Benchmark):
Provided:

- mappings d_i and trade-off parameters $\lambda_i > 0, i \in \mathcal{I}$
- estimated price $w \in \mathbf{R}_+^{|\mathcal{T}|}$,

$$\text{Solve:} \quad \underset{s_{\mathrm{c},i},\, i \in \mathcal{I},}{\text{minimize}} \quad \sum_{i \in \mathcal{I}} \left(\langle w, \mathrm{Re}(s_{\mathrm{c},i}) \rangle + \lambda_i d_i(\tilde{s}_{\mathrm{c},i}) \right). \tag{22}$$

The benchmark could be considered a contemporary strategy, where individual consumers considers only private objectives.

IV. Distributed Consumption Balancing

The framework for distributed coordination builds on the approaches derived in [5], [6]. It relies on ADMM, [7], [12].

First, we introduce auxiliary variables $z_j(t)$, $w_{\mathrm{l},j}(t)$, $w_{\mathrm{r},j}(t) \in \mathbf{C}$, for $j \in \mathcal{J}, t \in \mathcal{T}$, and define extended value function

$$g(w_{\mathrm{r},j}, \{w_{\mathrm{l},h} | h \in \mathrm{Ch}(j)\}, z_j) = \begin{cases} 0, & z_j \in \mathcal{V} \wedge w_{\mathrm{r},j} = \displaystyle\sum_{h \in \mathrm{Ch}(j)} w_{\mathrm{l},h} \\ \infty, & \text{otherwise.} \end{cases}$$

Using the above mappings, and by adding consistency constraints, (21) may be equivalently formulated

$$\begin{aligned} \underset{\substack{s_{\mathrm{c},i},\, s_{\mathrm{l},j},\, s_{\mathrm{r},j},\, u_{\mathrm{r},j} \\ w_{\mathrm{l},j},\, w_{\mathrm{r},j},\, z_j \\ i \in \mathcal{I},\, j \in \mathcal{J}}}{\text{minimize}} \quad & \sum_{i \in \mathcal{I}} c_{\mathrm{e}}(i, s_{\mathrm{l},i}, s_{\mathrm{c},i}) + \sum_{j \in \mathcal{J} \setminus \mathcal{I}} c_{\mathrm{l}}(j, s_{\mathrm{l},j}, s_{\mathrm{r},j}) \\ & + \sum_{j \in \mathcal{J}} g(w_{\mathrm{r},j}, \{w_{\mathrm{l},h} | h \in \mathrm{Ch}(j)\}, z_j) \\ \text{subject to} \quad & s_{\mathrm{l},t} = w_{\mathrm{l},t}, \quad s_{\mathrm{r},t} = w_{\mathrm{r},t}, \\ & P v_{\mathrm{r},t} = z_t, \\ & v_{\mathrm{r},t} = z_t - D_{\mathrm{p}} \mathrm{Re}(s_{\mathrm{l},t}) - D_{\mathrm{q}} \mathrm{Im}(s_{\mathrm{l},t}). \end{aligned} \tag{23}$$

All variables are complex, however, each constraint can be decomposed into separate constraints of the real and imaginary part *e.g.*

$$s_{\mathrm{l},j}(t) = w_{\mathrm{l},j}(t) \Leftrightarrow \begin{cases} \mathrm{Re}(s_{\mathrm{l},j}(t)) = \mathrm{Re}(w_{\mathrm{l},j}(t)) \\ \mathrm{Im}(s_{\mathrm{l},j}(t)) = \mathrm{Im}(w_{\mathrm{l},j}(t)) \end{cases}$$

By defining

$$F = \begin{bmatrix} I & & \\ & I & \\ & & P \end{bmatrix} \quad \begin{aligned} G_1 &= [\mathrm{Re}(D_p) \ \mathbf{0} \ I] \quad H_1 = [\mathrm{Re}(D_q) \ \mathbf{0} \ \mathbf{0}] \\ G_2 &= [\mathrm{Im}(D_p) \ \mathbf{0} \ \mathbf{0}] \quad H_2 = [\mathrm{Im}(D_q) \ \mathbf{0} \ I] \end{aligned}$$

and $I_0 = [\mathbf{0} \ \ \mathbf{0} \ \ I], I_+ = \mathrm{diag}(I, I, I)$, the constraints in (23) are equivalent to

$$\underbrace{\begin{bmatrix} F & \\ & F \\ G_1 & H_1 \\ G_2 & H_2 \end{bmatrix}}_{A} \underbrace{\begin{bmatrix} \mathrm{Re}(s_l(t)) \\ \mathrm{Re}(s_r(t)) \\ \mathrm{Re}(v_r(t)) \\ \mathrm{Im}(s_l(t)) \\ \mathrm{Im}(s_r(t)) \\ \mathrm{Im}(v_r(t)) \end{bmatrix}}_{\zeta(t)} + \underbrace{\begin{bmatrix} -I_+ & \\ & -I_+ \\ -I_0 & \\ & -I_0 \end{bmatrix}}_{B} \underbrace{\begin{bmatrix} \mathrm{Re}(w_l(t)) \\ \mathrm{Re}(w_r(t)) \\ \mathrm{Re}(z(t)) \\ \mathrm{Im}(w_l(t)) \\ \mathrm{Im}(w_r(t)) \\ \mathrm{Im}(z(t)) \end{bmatrix}}_{\eta(t)} = 0$$

for $t \in \mathcal{T}$, where $\zeta(t), \eta(t)$ are introduced simply to condense the notation in the following. Let

$$\zeta = (\zeta(1), \ldots, \zeta(N)), \quad \eta = (\eta(1), \ldots, \eta(N)),$$

then, by the definition of $\zeta(t)$ and $\eta(t)$ above, we let

$$c(\zeta) = \sum_{i \in \mathcal{I}} c_{\mathrm{e}}(i, s_{\mathrm{l},i}, s_{\mathrm{c},i}) + \sum_{j \in \mathcal{J} \setminus \mathcal{I}} c_{\mathrm{l}}(j, s_{\mathrm{l},j}, s_{\mathrm{r},j})$$

$$g(\eta) = \sum_{j \in \mathcal{J}} g(w_{\mathrm{r},j}, \{w_{\mathrm{l},h} | h \in \mathrm{Ch}(j)\}, z_j)$$

whereby (23) is equivalently expressed as

$$\begin{aligned} \underset{\zeta, \eta}{\text{minimize}} \quad & c(\zeta) + g(\eta) \\ \text{subject to} \quad & A\zeta(t) + B\eta(t) = 0, \quad t \in \mathcal{T}. \end{aligned}$$

This equivalent expression of (23) is now on the standard ADMM form [7], and may be solved iteratively by the following sequential updates of each set of variables:

$$\zeta^{k+1} = \arg\min_{\zeta} \left\{ c(\zeta) + \sum_{t \in \mathcal{T}} \frac{\rho}{2} \| A\zeta(t) + B\eta^k(t) + \mu^k(t) \|_2^2 \right\} \tag{24}$$

$$\eta^{k+1} = \arg\min_{\eta} \left\{ g(\eta) + \sum_{t \in \mathcal{T}} \frac{\rho}{2} \| \gamma^{k+1}(t) + B\eta(t) + \mu^k(t) \|_2^2 \right\} \tag{25}$$

$$\mu^{k+1}(t) = \mu^k(t) + \gamma^{k+1}(t) + B\eta^{k+1}(t) \quad t \in \mathcal{T}, \tag{26}$$

where $\gamma^{k+1}(t) = \alpha A\zeta^{k+1}(t) - (1 - \alpha)B\eta^k(t)$. Above, k is an iteration index, and should not be read as an exponent. The quantity $\mu(t)$ is the Lagrange multipliers for the equality constraints scaled by ρ. The iterates start from some initial guess ζ^0, η^0 and μ^0. The parameters $\rho > 0$ and $\alpha \in [1, 2)$ are design parameters of the algorithm and are known as the ADMM parameter and over-relaxation parameter [13]. These affect the convergence speed of the algorithm. A method for picking suitable values for these parameters is still an open-ended question, although [13] presents some results for specific classes of problems.

Termination of the algorithm is based on the residuals

$$\begin{aligned} \xi^{k+1}(t) &= A\zeta^{k+1}(t) + B\eta^{k+1}(t) \\ \psi^{k+1}(t) &= \rho A^T B(\eta^{k+1}(t) - \eta^k(t)), \end{aligned} \tag{27}$$

known as the primal and dual residuals [7]. Choosing some absolute tolerance ϵ_{abs}, the algorithm is stopped when

$$\max(\|\xi^{k+1}\|_2, \|\psi^{k+1}\|_2) \leq \sqrt{6(n+b)T}\,\epsilon_{\mathrm{abs}}, \tag{28}$$

where the scaling by $\sqrt{6(n+b)T}$ is simply to account for problem size.

The reader is referred to [7], [12], for proofs of convergence for the ADMM algorithm. For our purposes, it suffices to mention that the algorithm converges both in cost and feasibility, *i.e.*

$$c(\zeta^k) + g(\eta^k) \to \phi^\star, \quad \|\xi^k\|_2 \to 0, \quad \text{as} \quad k \to \infty.$$

The following describes how the updates (24)-(26) renders a coordination strategy relying only on distributed information sharing.

Interpretation as neighbor based communication

Observe that all elements of the cost function in (23) are separable, *i.e*, there are no shared variables. The complicating factors only appear due to constraints. Notice also that the constraints $A\zeta(t) + B\eta(t) = 0$ can be explicitly formulated

$$v_{\mathrm{r},j} + (r_j + \mathrm{j}x_j)\mathrm{Re}(s_{\mathrm{l},j}) + (x_j - \mathrm{j}r_j)\mathrm{Im}(s_{\mathrm{l},j}) = z_j \quad (29)$$

$$s_{\mathrm{l},j} = w_{\mathrm{l},j}, \quad s_{\mathrm{r},j} = w_{\mathrm{r},j}, \quad (30)$$

$$v_{\mathrm{r},j} = z_h, \quad h \in \mathrm{Ch}(j), \quad j \in \mathcal{J}. \quad (31)$$

As discussed in Section I, the coordination procedure of this work is designed for at future grid, where an advanced metering and control infrastructure is available. For this reason, we assume that each consumer in the grid has a local dedicated computation device, as does each cable section and grid junction. In a practical setup, some of these private computation devices may physically be the same, however, we shall treat them individually in the following. We let

$$(s_{\mathrm{l},i}, s_{\mathrm{c},i}, v_{\mathrm{r},i}), \quad i \in \mathcal{I},$$

be private variables of each consumer, and appertaining leaf. Correspondingly, we let $(s_{\mathrm{l},j}, s_{\mathrm{r},j}, v_{\mathrm{r},j})$, $j \in \mathcal{J}\backslash\mathcal{I}$, be private variables of each branch. The private variables are governed by the dedicated computation device of each consumer or cable. Similarly, we assign private variables

$$(w_{\mathrm{r},j}, \{w_{\mathrm{l},h} | h \in \mathrm{Ch}(j)\}, z_j), \quad j \in \mathcal{J},$$

to each bus-bar. We further assign the lagrange multiplier associated to the each constraint, as a private variable of the corresponding busbar.

Notice in (29)-(31) that we have written all variables private to node j on the left of the equalities, and all variables external to node j on the right. From this it can be seen that in order to make ζ-update (24), each branch and leaf $j \in \mathcal{J}$ needs to be provided values

$$(w^k_{\mathrm{r},j}(t), w^k_{\mathrm{l},j}(t), z^k_j(t), \{z^k_h(t) | h \in \mathrm{Ch}(j)\}),$$

along with the current value of the associated lagrange multipliers. That is, the current ADMM variables and lagrange multipliers must be forwarded, but only from the immediate bus-bar, and the parent and children bus-bars, as illustrated in Fig. 4(left). In the figure, each arrow represents a set of variables being communicated from one point in the grid to another. The arrow base indicates where the variables are stored, whereas the arrow head indicates where they are communicated to.

Similarly, in order to conduct the η-update of the auxiliary variables in (25), and subsequently the lagrange update in (26), each bus-bar $j \in \mathcal{J}$ needs only the values

$$(s^{k+1}_{\mathrm{r},j}, \{s^{k+1}_{\mathrm{l},h} | h \in \mathrm{Ch}(j)\}, v^{k+1}_{\mathrm{r},j}, v^{k+1}_{\mathrm{r,Pa}(j)}),$$

which again needs only local data to be passed around as illustrated in Fig. 4(right). From this it is apparent that the approach outlined here requires only local data to be passed around, whereby the need for a central governor or controller is avoided.

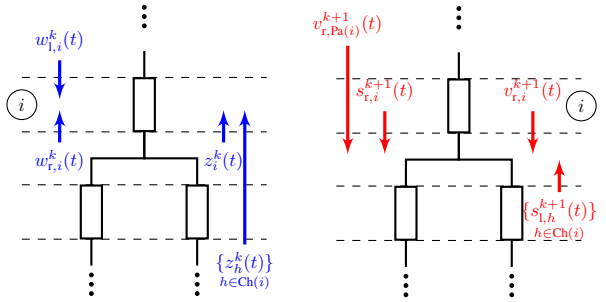

Fig. 4. **Left:** Data passing prior to ζ-update: In order for the i^{th} cable section to update private variables, it needs the current ADMM and lagrange variables from the neighboring nodes in the grid. The lagrange variables are not explicitly drawn in the figure, since they are each associated to one of the existing arrows. **Right:** Corresponding data passing prior to η-update of the i^{th} bus-bar.

V. Numerical Example

The following numerical example demonstrates the coordination approach. The example spans a 24 hour horizon starting at 8 AM, divided into 1 hour samples. We coordinate a network containing $n = 34$ consumers and $b = 11$ branches, corresponding in size to the benchmark network examined in [4]. The topology of the network is presented in Fig. 5. The estimated price-signal, solar generated power production and baseline consumption, used in the coordination, are presented in Fig. 6, in per-unit (pu) measures with base values of 1 kVA and 400 V for power and voltage respectively.

The price signal is provided in a generalized currency (¤/pu). Solar power is presented as a average curve, from which each individual consumer will exhibit some randomly generated deviations. The reactive baseline consumption is derived from the active, by use of a constant power factor of 0.9 lagging, for all consumers. Flexible appliances are distributed at random between consumers, such that each consumer has a 90 % chance of having an appliance, with equal probability of the appliance being either, an EHP, EV or PV. From this assignment procedure, the following example includes 7 EHPs, 10 EVs, and 10 PVs.

The voltage variation constraint has been set to 0.08 pu. The actual limit in the Danish system is 0.1 pu [2]. However, as we employ an approximate model, a tighter bound allows for some deviation. The grid impedances resemble those employed in [2], scaled to give a baseline loss around 3 %.

We conduct the coordination employing the distributed

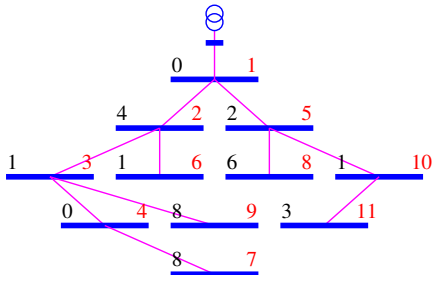

Fig. 5. Tree structure of the electrical grid. The horizontal lines represents bus-bars and vertical or sloping lines, represents branch cables. Consumers and leaves are not drawn explicitly. The number to the left of each bus-bar represents the number of consumers connected to that point in the grid, whereas the right number refer to the ordering of the bus-bars.

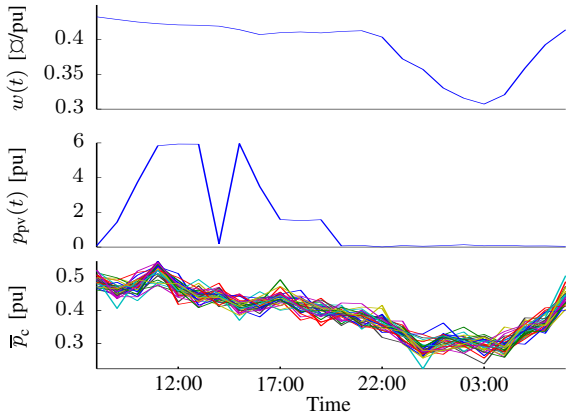

Fig. 6. **Top:** Estimated electricity price. **Middle:** Estimated solar power production. **Bottom:** Estimated Baseline consumption.

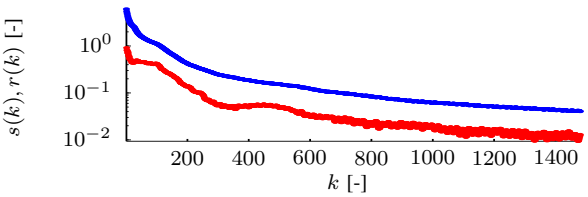

Fig. 7. Convergence of the primal (top), and dual residuals (bottom).

strategy derived in the preceding sections. As this example is fairly small, a centralized solution can also be obtained, giving the global optimum for comparison.

In the distributed coordination scheme, we employ parameter values $\rho = 0.1$ and $\alpha = 1.9$ which appears to work well for this problem. We set the absolute residual termination tolerance as $\epsilon_{\text{abs}} = 5\text{E-}4$. It has been experienced that the quadratic, relaxed, loss constraint in (9) is very computationally demanding in simulations. To improve computation speed we have in this example approximated the quadratic map (7) as a piecewise affine function:

$$z_j l(u,y)(t) \approx l_j^{\text{appr}}(u,y)(t) = \max\left(H_j \begin{bmatrix} u(t) \\ y(t) \end{bmatrix} + g_j\right), \quad j \in \mathcal{J} \tag{32}$$

where $H_j \in \mathbf{R}^{K\times 2}, g_j \in \mathbf{R}^K$ are the coefficients of the approximation, and $K \in \mathbf{N}$ is the number of affine functions used in the approximation. This approximation is included as the implicit constraint in (10).

The convergence of ADMM for this example is presented in Fig. 7, showing that termination accuracy is obtained after roughly 1500 iterations. The primal residuals decrease in a fairly even way, whereas the dual residuals exhibit substantially more variation. These variations have not been explored in depth, however we speculate that this behavior relates to the inertia of the ADMM method, inherited from the way past iterations influence future updates. This is due to the resemblance to the variations investigated in [14].

Upon termination of the distributed algorithm, the coordinated power consumption appears as in Fig. 8, where the centrally found global optimum is also presented. As evident, the distributed solution is almost indistinguishable from the global optimum, and the cost of the decentralized solution deviates from that of the global optimum by only 2.3E-3 %.

The voltage magnitude is presented in Fig. 9, showing the correspondence between the voltage profiles found by the distributed algorithm, and the actual true voltage profiles found by Gauss-Seidel load flow analysis, when employing the coordinated consumption profiles in Fig. 8. Despite the approximations introduced in Equation (5), the maximum voltage error is only of 0.28 %.

The total loss error when comparing the losses found by the dirstributed algorithm, and those found by load flow analysis, accumulates to 10.7 %. This is partly due to the crudeness of the affine approximation introduced in (32), but is mainly caused by the voltage approximation $v_{\text{r},j} \approx v_{\text{l},j} \approx 1$ introduced in (4) and (6). It has been experienced that the loss error can be greatly reduced by employing a more educated guess of the voltage, *e.g.* based in historical measurements.

The flexible consumption profiles obtained through coordination are shown in Fig. 10, along with those obtained by the benchmark strategy. As evident from Fig. 10(top), there is not much difference between the consumption of EHPs in the benchmark and coordinated case. This is because the set-point tracking embedded in the discomfort measure in (13) naturally distributes the EHP consumption over time. This implicitly decreases the losses, rendering no benefit to be obtained by introducing temporal shifts. In that regard, the distributed coordination strategy derived here, arrives at similar results as disucssed by [4].

For EVs on the other hand, there is a large difference between the benchmark and coordinated case, Fig. 10(Middle). In the benchmark case, the optimal charge schedule is fairly obvious, since the vehicle should be fully charged during low-price periods, and fully discharge during high-price periods, in a fashion that leaves the vehicle fully charged at the end of the horizon. In this way it is possible for the EV owner to make money by selling energy back to the grid. This would however cause significant over and under voltages, and incur massive losses. In the coordinated case, the charging of vehicles is much more distributed across the horizon, in order to accommodate the cost of losses, and to satisfy voltage constraints. This is more clearly visible in Fig. 11, where the accumulated EV consumption is plotted. Here it is clear

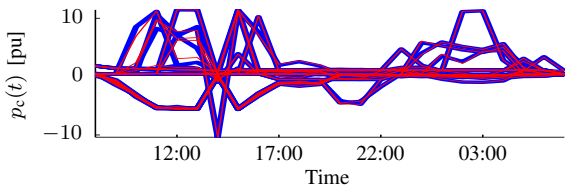

Fig. 8. The coordinated consumption pattern found centralized (Red), and distributed (Blue).

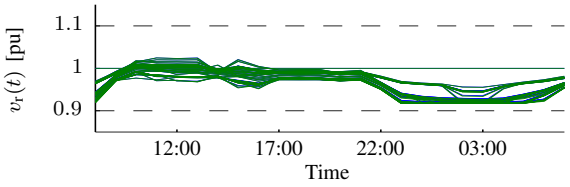

Fig. 9. The approximated voltage profiles found during distributed coordination (Blue), and the true voltage profiles calculated by load flow analysis (Green).

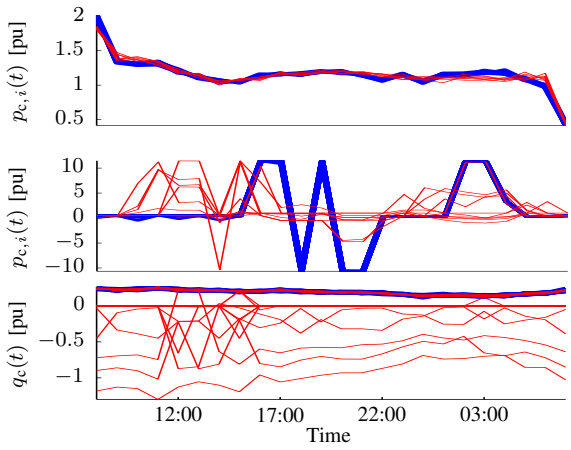

Fig. 10. **Top:** The active power consumption pattern for $i \in \mathcal{I}_{\text{ehp}}$ in the coordinated case (Red) and the benchmark case (Blue). **Middle:** Similar to the above, for $i \in \mathcal{I}_{\text{ev}}$. **Bottom:** Similar as above, for reactive consumption of all consumers.

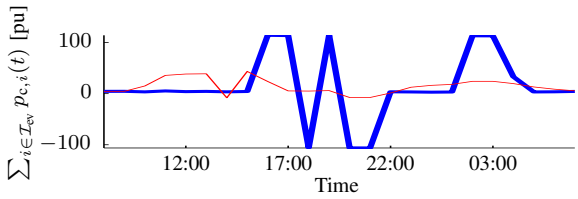

Fig. 11. Accumulated consumption of EVs at each time step, using the benchmark strategy (Blue), and the distributed coordination (Red).

that the benchmark strategy gives a bang-bang charge and discharging of vehicles, whereas the charging is smoothed out when it is coordinated. The main charge period in the coordinated case is in the beginning of the horizon, which is in fact to absorb the locally produced solar power visible in Fig. 6(middle), rather than introducing losses by first exporting the solar power, and later importing power for charging. This is not a concern in the benchmark case. Finally in Fig. 10(bottom), the reactive consumption is presented for all consumers, where we remark that negative consumption corresponds to production of reactive power. From the figure it is clear that consumers with reactive capabilities either balance their own reactive baseline consumption such that their local reactive power flow is zero, or an amount of reactive power is produced, in order to accommodate the consumption of consumers without reactive capabilities.

VI. Conclusion and Perspectives

In this paper we have extended results from previous works, and illustrated how voltage control can be included in coordination framework of the of flexible energy consumption of residential consumers. The voltage control has been included in a way that requires no central control unit, and allows for a completely distributed optimization, where communication with neighbors is the only requirement. Our framework includes a detailed model of the electrical grid, and includes concerns towards losses as an objective in the coordination, along with private objectives for each consumer in the grid. Numerical results have shown how our distributed framework converges towards the global optimum of the posed problem, and we have demonstrated how various flexible appliances may contribute differently to the coordination.

Although not implemented, the framework presented for tree-structured graphs, does allow for distributed termination of the coordination: Each node in the network is able to evaluate their local residuals (27), and locally estimate if the termination criterion (28) is satisfied. If any node has received 'satisfied' notifications from all its children, and if the node itself also estimates that the termination criterion is satisfied, it may send a 'satisfied' notification to its own parent as well. In this way, local satisfaction can propagate from the leafs towards the root, which can ultimately decide to terminate the algorithm.

For the sake of brevity, various relevant concerns have been disregarded in this work, but may readily be included with little or no changes to the framework. This includes local capacity constraints on power transport of each cable, preferred charge schedules of EVs, penalties for charge variations, *etc*.

Acknowledgement

This work is supported by the Southern Denmark Growth Forum and the European Regional Development Fund, under the project "Smart & Cool". The authors greatly appreciate the inputs and comments of Euhanna Ghadimi, KTH, and Christoffer Sloth, AAU, during technical discussions.

References

[1] T. Pedersen, P. Andersen, K. Nielsen, H. Stærmose, and P. Pedersen, "Using heat pump energy storages in the power grid," *IEEE Conference on Control Applications, Proceedings*, 2011.

[2] J. Pillai, P. Thøgersen, J. Møller, and B. Bak, "Integration of electric vehicles in low voltage Danish distribution grids," *Power and Energy*, 2012.

[3] M. Juelsgaard, P. Andersen, and R. Wisniewski, "Distribution loss reduction by household consumption coordination in smart grids," *IEEE Transactions on Smart Grid*, vol. 5, no. 4, pp. 2133–2144, 2014.

[4] M. Juelsgaard, C. Sloth, R. Wisniewski, and J. Pillai, "Loss minimization and voltage control in smart distribution grid," *Proceedings of the IFAC World Congress*, 2014, To appear.

[5] M. Kraning, E. Chu, J. Lavaei, and S. Boyd, "Dynamic network energy management via proximal message passing," *Foundations and Trends in Optimization*, vol. 1, no. 2, pp. 73–126, 2014.

[6] P. Šulc, S. Backhaus, and M. Chertkov, "Optimal distributed control of reactive power via the alternating direction method of multipliers," pp. 26–37, Oct. 2013, unpublished, Available at arxiv: *www.arxiv.org/abs/1310.5748*.

[7] S. Boyd, N. Parikh, E. Chu, B. Peleato, and J. Eckstein, "Distributed optimization and statistical learning via the alternating direction method of multiplier," *Foundations and Trends in Machine Learning*, vol. 3, no. 1, 2010.

[8] P. Kundur, *Power system stability and control*. McGraw-Hill, 1993.

[9] C. Desoer and E. Kuh, *Basic Circuit Theory*. McGraw-Hill, 2010.

[10] V. Monteiro, J. Pinto, B. Exposto, H. Goncalves, J. Ferreira, C. Couto, and J. Afonso, "Assessment of a battery charger for electric vehicles with reactive power control," *IEEE Industrial Electronics Society annual conference*, pp. 5142–5147, Oct. 2012.

[11] K. Turitsyn, P. Sulc, S. Backhaus, and M. Chertkov, "Options for Control of Reactive Power by Distributed Photovoltaic Generators," *Proceedings of the IEEE*, vol. 99, no. 6, pp. 1063–1073, Jun. 2011.

[12] D. Bertsekas and J. Tsiksiklis, *Parallel and Distributed Computation: Numerical Methods*. Athena, 1997.

[13] E. Ghadimi, A. Teixeira, I. Shames, and M. Johansson, "Optimal parameter selection for the alternating direction method of multipliers (admm): quadratic problems," Jun. 2013, available from Arxiv: *www.arxiv.org/abs/1306.2454*.

[14] B. O'Donoghue and E. Candés, "Adaptive restart for accelerated gradient schemes," *Foundations of Computational Mathematics*, 2013.